AN ALTERNATIVE THEORY OF TRANSIT-TIME OSCILLATIONS IN HALL THRUSTERS

Serge Barral, Zbigniew Peradzyński*, Karol Makowski
Institute of Fundamental Technological Research - PAS
Świętokrzyska 21, 00049 Warsaw, Poland
*also: Warsaw University, Mathematics Dept., Warsaw, Poland
sbarral@ippt.gov.pl, zperadz@ippt.gov.pl, kmak@ippt.gov.pl

Michel Dudeck
CNRS Laboratoire d'Aérothermique
45071 Orléans, France
dudeck@cnrs-orleans.fr

Abstract

The longitudinal oscillations highlighted by numerical models of Hall thrusters in the range $100 - 500$ kHz own several characteristics that are reminiscent of the so-called transit-time oscillations observed experimentally. The corresponding dispersion relation is derived from one-dimensional ion transport equations, assuming a constant discharge current. It correctly anticipate the presence of two distinct unstable regions in the near-anode region and in the acceleration region. The role of the ionization degree on the stability and the close relationship between the phase velocity and the ion velocity both support the hypothesis that this oscillation mode is indeed the counterpart of the transit-time instability observed in experiments. As a corollary, an effective mean of suppressing this instability in numerical models without affecting low-frequency modes is outlined.

1 Introduction

Transit-time oscillations have been experimentally characterized by A. I. Morozov *et al.* as longitudinal plasma oscillations whose frequency is approximately inversely proportional to the time of flight of ions inside the channel [1, 2]. Their apparition has been found to be mostly conditioned by a high degree of ionization, either resulting from the use of an easily ionized gas or from a high discharge voltage.

Interestingly, high frequency oscillations propagating with the velocity of ions have been repeatedly observed in kinetic, hybrid and fluid models of Hall thrusters [3, 4, 5, 6], exhibiting features that strongly remind the experimental transit-time instability. Although these oscillations were first believed to be a simulation artifact [3], it has now become clear that they do neither depend on the modeling paradigm nor on the numerical mesh, thus ruling out the possibility of a numerical instability. The prediction of such oscillations in numerical simulations of SPT-100 type thrusters remains nevertheless intriguing, as no such instabilities have been reported to date in such engines.

Although a stability criterion for transit-time oscillations has been proposed [7], its validity was later strongly questioned [8] and the impact of the ionization degree has remained unexplained. Besides, the apparent absence of transit-time instabilities in modern Hall thrusters strongly challenges the predicted relationship between unstable modes and sharp magnetic field gradient. Notwithstanding the former concerns, it is acknowledged that this theory is not adequate to describe the instability exhibited by numerical models [5].

2 Manifestation in numerical models

Although the discussion below is mostly based on the results of a one-dimensional fluid model of Hall thruster, other authors have shown that the main characteristics of this instability do not strongly depend upon the underlying numerical scheme [4]. We shall thus omit here the description of the fluid model, which can be found elsewhere [9, 10].

The numerical transit-time instability results in very strong oscillations of the local plasma parameters (plasma density, ion velocity, electron temperature, ...) and of the discharge current. The amplitude of discharge current oscillations may be superimposed on the low-frequency (so-called "breathing-mode") oscillations, as shown by figure 2. Surprisingly enough, transit-time oscillations are still recovered and preserve the same characteristics when a constant discharge current is prescribed instead of a constant discharge voltage. In most cases, transit-time oscillations are confined to the ion acceleration region, where the magnetic field is high, but small oscillations may also be observed in the near-anode region in some circumstances.

The evolution of the ion density and velocity in a case where both regions are unstable is shown on figure 1. Let us emphasize that on this example, the discharge current was prescribed: otherwise stable regions would still fluctuate due to the global influence range of discharge current oscillations.

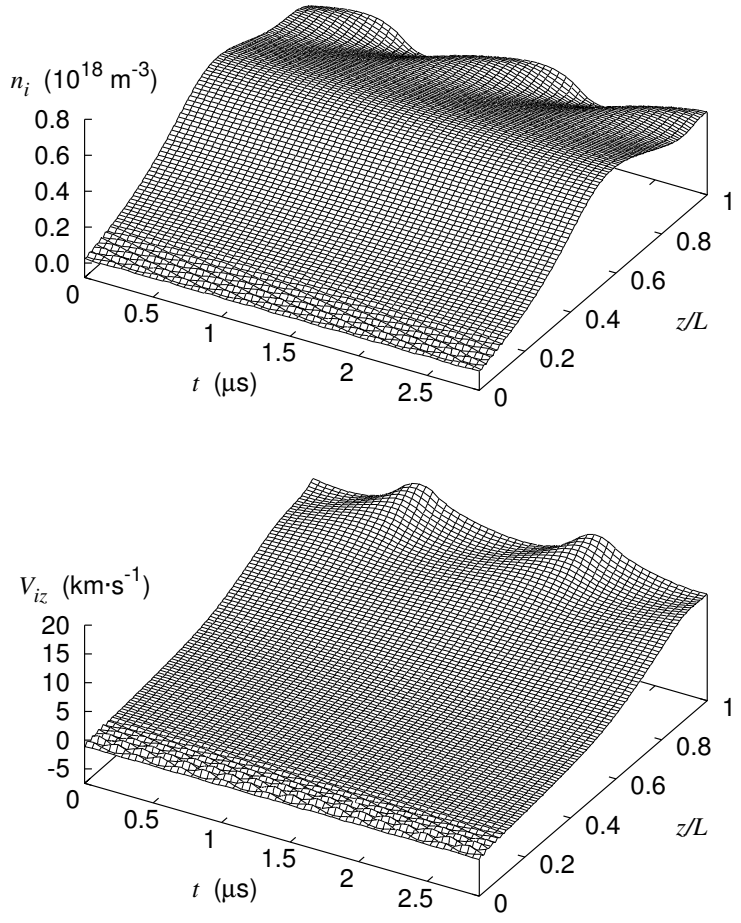

FIGURE 1: Simulated transit-time oscillations of ion density and ion velocity from simulations, for a prescribed discharge current ($I_d = 3$ A).

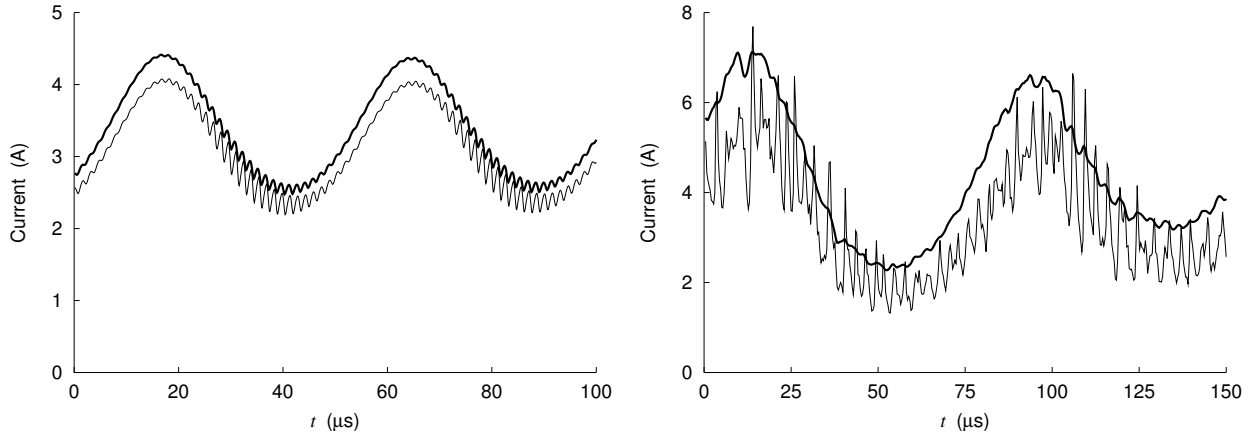

FIGURE 2: Typical samples of simulated discharge current (thick lines) and ion current at the exhaust (thin lines) when transit-time oscillations are superimposed on low frequency oscillations. Left: results obtained with a fluid model [9, 10]. Right: results obtained with a hybrid model by G. J. M. Hagelaar, J. Bareilles, L. Garrigues and J.-P. Boeuf [5].

3 Stability study

3.1 Governing equations

A dispersion relation for the transit-time instability can be derived from the continuity and momentum equation for cold ions:

$$\frac{\partial n_i}{\partial t} + \frac{\partial \left(n_i V_{iz}\right)}{\partial z} = \nu_i \, n_e \tag{1}$$

$$\frac{\partial \left(n_i V_{iz}\right)}{\partial t} + \frac{\partial \left(n_i V_{iz}^2\right)}{\partial z} = \frac{e \, E_z}{m_i} \, n_i \tag{2}$$

where m_i, n_i and V_{iz} are respectively the mass, density and axial velocity of ions, n_e is the density of electrons, ν_i is the ionization frequency, and E_z the axial electric field. This electric field can then be evaluated from the generalized Ohm's law

$$V_{ez} = -\mu_e \left(E_z + \frac{\kappa T_e}{e \, n_e} \frac{\partial n_e}{\partial z} \right) \tag{3}$$

where μ_e is the axial electron mobility and V_{ez} the axial drift velocity of electrons. V_{ez} can in turn be eliminated using the conservation of the total current

$$I_d = I_i + I_e = eA \left(n_i V_i - n_e V_e \right) \tag{4}$$

where I_i and I_e are respectively the ion and electron currents, while A stands for the cross-section area of the channel.

After substitution of E_z in the ion momentum equations (2) and assuming quasi-neutrality (*i.e.* $n_e = n_i$), one obtains the following system:

$$\frac{\partial n_i}{\partial t} + \frac{\partial \left(n_i V_{iz}\right)}{\partial z} = \nu_i \, n_i \tag{5}$$

$$\frac{\partial \left(n_i V_{iz}\right)}{\partial t} + \frac{\partial \left(n_i V_{iz}^2\right)}{\partial z} + \frac{\kappa T_e}{m_i \, n_e} \frac{\partial n_i}{\partial z} = n_i \frac{e}{m_i} \frac{1}{\mu_e} \left(\frac{I_d}{A \, e \, n_i} - V_{iz} \right) . \tag{6}$$

3.2 Dispersion relation

The ion density and velocity are linearized around a stationary state (n_{i0}, V_{iz0}), expressing the perturbed quantities as

$$n_i = n_{i0} + n_{i1} \exp\left[\mathrm{j}\left(k\,z - \omega\,t\right)\right] \tag{7}$$

$$V_{iz} = V_{iz0} + V_{iz1} \exp\left[\mathrm{j}\left(k\,z - \omega\,t\right)\right]\ . \tag{8}$$

where n_{i0} and V_{iz0} verify

$$\frac{d\left(n_{i0}V_{iz0}\right)}{dz} = \nu_i\, n_{i0} \tag{9}$$

$$\frac{d\left(n_{i0}V_{iz0}^2\right)}{dz} + \frac{\kappa T_e}{m_i\, n_e}\frac{dn_{i0}}{dz} = n_{i0}\frac{e}{m_i}\frac{1}{\mu_e}\left(\frac{I_d}{A\,e\,n_{i0}} - V_{iz0}\right)\ . \tag{10}$$

It is clear from figure 2 that the discharge current is much less affected by transit-time oscillations than the ion current. Therefore, we consider all parameters but n_i and V_{iz} constant in the system (5, 6). After linearization, the following dispersion relation is obtained:

$$\omega^2 + \omega\left(-2k\,V_{iz} + \mathrm{j}\,\mathcal{A}\right) + \mathcal{B} + k^2V_{iz}^2\left(1 - \frac{1}{\mathcal{M}_i}\right) + \mathrm{j}\,k\,V_{iz}\,\mathcal{C} = 0 \tag{11}$$

where the isothermal ion sound velocity and ion Mach number are respectively given by

$$C_s = \sqrt{\frac{\kappa T_e}{m_i}}\,, \tag{12}$$

$$\mathcal{M}_i = \frac{V_{iz}}{C_s}\,, \tag{13}$$

while other coefficients can be simplified as follows, using equations (9, 10):

$$\mathcal{A} = \frac{2}{1-\alpha}\left\{\nu_i + \Delta\nu\left[1 - \frac{\alpha}{2} + (1-\alpha)\,Y\right]\right\}\ , \tag{14}$$

$$\mathcal{B} = \frac{2}{1-\alpha}\left\{-\Delta\nu^2\left[1 + (2-\alpha)\,Y + (1-\alpha)\,Y^2\right] - 2\nu_i\Delta\nu\,(1+Y)\right\}\ , \tag{15}$$

$$\mathcal{C} = -\Delta\nu\,(1+2Y)\ , \tag{16}$$

with

$$Y = \frac{1}{\mathcal{M}_i^2 - 1}\,, \tag{17}$$

$$\alpha = \frac{I_i}{I_d} = \frac{e\,A\,n_iV_{iz}}{I_d}\,, \tag{18}$$

$$\Delta\nu = \frac{1-\alpha}{\alpha}\frac{e}{m_i}\frac{1}{\mu_e} - 2\nu_i\,. \tag{19}$$

The solution of equation (11) is

$$\omega = k\,V_{iz} - \mathrm{j}\frac{\mathcal{A}}{2} \pm \frac{1}{\sqrt{2}}\left[\sqrt{\sqrt{\left(k^2C_s^2 + \mathcal{Q}\right)^2 + k^2V_{iz}^2\mathcal{R}^2} + \mathcal{Q} + k^2C_s^2}\right.$$
$$\left. + \mathrm{j}\,\varepsilon\sqrt{\sqrt{\left(k^2C_s^2 + \mathcal{Q}\right)^2 + k^2V_{iz}^2\mathcal{R}^2} - \left(k^2C_s^2 + \mathcal{Q}\right)}\right]\ , \tag{20}$$

with

$$\varepsilon = \begin{cases} 1 & \text{if} \quad k\,V_{iz}\mathcal{R} > 0 \\ -1 & \text{if} \quad k\,V_{iz}\mathcal{R} < 0 \end{cases} \tag{21}$$

and

$$\mathcal{Q} = -\left(\frac{\mathcal{A}^2}{4} + \mathcal{B}\right) , \tag{22}$$

$$\mathcal{R} = -\left(\mathcal{A} + \mathcal{C}\right) = -\frac{1}{1-\alpha}\left(2\nu_i + \Delta\nu\right) = -\frac{1}{\alpha}\frac{e}{m_i}\frac{1}{\mu_e} . \tag{23}$$

4 Analysis of the short-wave behavior

4.1 Validity of the asymptotic short-wave behavior.

Since the dispersion relation was derived from a linearization around the local state, the long-wave behavior ($k \to 0$) is meaningless. Fortunately, much insight can be gained from a study of the asymptotic short-wave limit ($k \to \infty$). Indeed, the growth rate obtained from equation (20) is characterized by a monotonic behavior and quickly saturates above some critical value of k, so that the behavior for $k \to \infty$ actually defines most of the unstable spectrum. Defining for instance a critical wavenumber

$$k_c = \frac{1}{C_s}\sqrt{\frac{\mathcal{M}_i^2\mathcal{R}^2}{2} + 2\,|\mathcal{Q}|} \tag{24}$$

it can be shown that the growth rate satisfies

$$\left|\frac{\mathrm{Im}\,\omega(\infty) - \mathrm{Im}\,\omega(k)}{\mathrm{Im}\,\omega(\infty) - \mathrm{Im}\,\omega(0)}\right| < 0.202 \qquad \forall\, k \geq k_c\,, \tag{25}$$

which means that $\mathrm{Im}\,\omega(k)$ is already very close to saturation above k_c. The value $1/k_c$ is of the order of the characteristic length of plasma parameters gradients, *i.e.* it is in general of the order of the length of the device. Since wavenumbers larger than the extend of the device are not likely to occur, it can thus be expected that the asymptotic growth rate for $k \to \infty$ constitutes a reasonable approximation of the actual growth rate.

4.2 Phase velocity and frequency

In the short-wave limit, the phase velocity converges to

$$\lim_{k\to\infty}\left(\frac{\mathrm{Re}\,\omega}{k}\right) = V_{iz} \pm C_s\,. \tag{26}$$

If $\mathcal{Q}$ is negative (which is generally the case) the phase velocity satisfies additionally

$$V_{iz} - C_s < \frac{\mathrm{Re}\,\omega(k)}{k} < V_{iz} + C_s \qquad \forall\, k\,, \tag{27}$$

which confirms the observed correlation between the propagation velocity of the wave and the velocity of ions.

4.3 Frequency

The main frequency is theoretically determined by the wavenumbers associated with the highest growth rate. In the present case, the growth rate converges at high frequencies towards

$$\lim_{k\to\infty}\left(\mathrm{Im}\,\omega\right) = -\frac{\mathcal{A}}{2} \pm \left|\mathcal{M}_i\frac{\mathcal{R}}{2}\right| . \tag{28}$$

This behavior suggests that for $|\mathcal{M}_i\mathcal{R}| - \mathcal{A} > 0$, the unstable mode will be characterized by an infinitely wide frequency spectrum. In practice, however, high frequencies are damped by various diffusion processes. If for instance the actual equation system includes diffusion and dissipation terms weighted by a coefficient ξ:

$$\frac{\partial n_i}{\partial t} + \frac{\partial \left(n_i V_{iz}\right)}{\partial z} = \nu_i \, n_e + \xi \frac{\partial^2 n_i}{\partial z^2} \tag{29}$$

$$\frac{\partial \left(n_i V_{iz}\right)}{\partial t} + \frac{\partial \left(n_i V_{iz}^2\right)}{\partial z} = \frac{e \, E_z}{m_i} \, n_i + \xi \frac{\partial^2 \left(n_i V_{iz}\right)}{\partial z^2} \, , \tag{30}$$

then the growth rate becomes

$$\mathrm{Im}\, \omega|_\xi = \mathrm{Im}\, \omega|_{\xi=0} - \xi k^2 \, . \tag{31}$$

Since the growth rate $\mathrm{Im}\, \omega|_{\xi=0}$ of the non-diffusive equation system rapidly stabilizes as $k \to \infty$, it is likely that the actual growth rate will present a maximum in the vicinity of the smallest possible wavenumber. Therefore, on may surmise that the most excited wavelength will be of the order of the length of the unstable region, that is of the order of the length L of the device. The main frequency characterizing the instability can thus be expected to scale as

$$f \approx \frac{V_i \pm C_s}{L} \, . \tag{32}$$

4.4 Stability criterion

4.4.1 General case

Using equations (9, 10), $\mathcal{A}$ can be rewritten as

$$\mathcal{A} = \frac{e}{m_i} \frac{1}{\mu_e} + 2 \frac{dV_{iz0}}{dz} \, . \tag{33}$$

Since the terms on the right hand side are both positive in normal circumstances, we shall assume that $\mathcal{A} > 0$ and derive from equation (28) the following stability criterion:

$$\frac{|\mathcal{M}_i\mathcal{R}|}{\mathcal{A}} < 1 \, . \tag{34}$$

4.4.2 Low ionization limit

In the case where ionization can be neglected, *i.e.* for

$$\nu_i \ll \frac{1-\alpha}{\alpha} \frac{e}{\mu_e m_i} \, , \tag{35}$$

the stability condition can be rewritten explicitly as

$$\frac{|\mathcal{M}_i|}{\left| 1 + \left(1 - \frac{I_i}{I_d}\right) \frac{\mathcal{M}_i^2 + 1}{\mathcal{M}_i^2 - 1} \right|} < 1 \, . \tag{36}$$

The stable and unstable regions predicted by equation (36) are shown on figure 3.

It must be emphasized that the low ionization hypothesis is necessarily violated at the sonic point, where the requirement of a smooth sonic transition transforms equation (35) into a strict equality. It was observed in simulations, however, that this hypothesis is by contrast reasonably justified in the subsonic region and very well justified in the supersonic (acceleration) region.

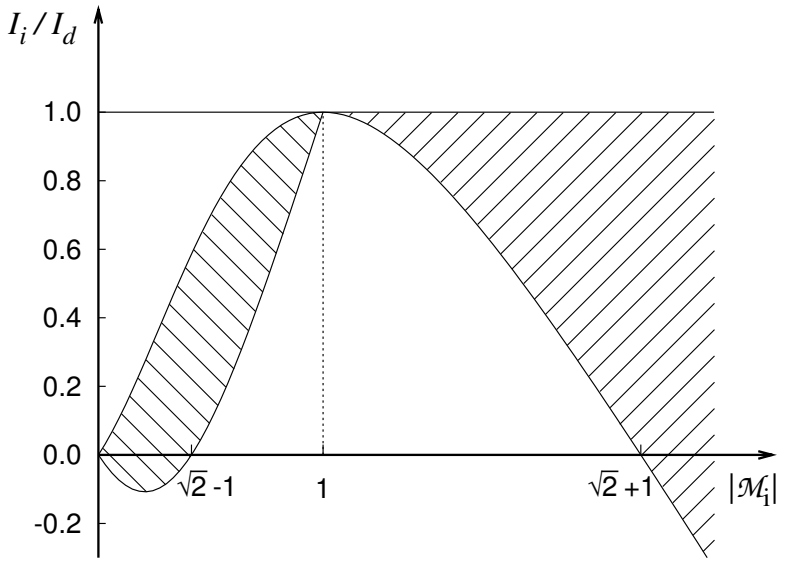

FIGURE 3: Stable (blank) and unstable (hatched) regions for the transit-time instability, neglecting ionization.

4.4.3 Effect of ionization

In the diffusion region ($|\mathcal{M}_i| \ll 1$), the effect of ionization can be qualitatively assessed from the low-Mach stability criterion, obtained in the limit $Y \to -1$:

$$\left|\frac{\mathcal{M}_i}{\alpha}\right| \frac{1}{1 + 2\,\dfrac{\mu_e m_i\,\nu_i}{e}} < 1\,. \tag{37}$$

This suggests that ionization actually tends to improve the local stability in the subsonic region. Note that remark concerns only the *local* effect of ionization, and does not hold for the ionization degree I_i/I_d at the point considered.

By contrast, the stability criterion obtained within the hypersonic approximation ($|\mathcal{M}_i| \gg 1$) reads

$$\left|\frac{\mathcal{M}_i}{\alpha}\right| \frac{1}{\dfrac{2-\alpha}{\alpha} - 2\,\dfrac{\mu_e m_i\,\nu_i}{e}} < 1$$

and highlights therefore a destabilizing effect due to ionization.

5 Discussion

5.1 Comparison with experiments

The maximum ion Mach number is in general reached close to the channel exhaust, and typically amounts to $1.5 - 2.5$. According to figure 3, if the maximum ion Mach number is such that $1 < \mathcal{M}_i < \sqrt{2} + 1$, the stability is ultimately dependent on the ionization degree. This prediction is in remarkable agreement with the experimental observation that gases with low ionization potential lead more often to instability, and that the transit-time instability is visible only in the current saturation region [2].

Besides, the fact that the growth rate is not a decaying function of the frequency [equation (28)] implies that transit-time oscillations should present a broad frequency spectrum, which is also consistent with experimental reports [1, 2] (the failure of numerical models to recover a broad frequency spectrum is discussed later).

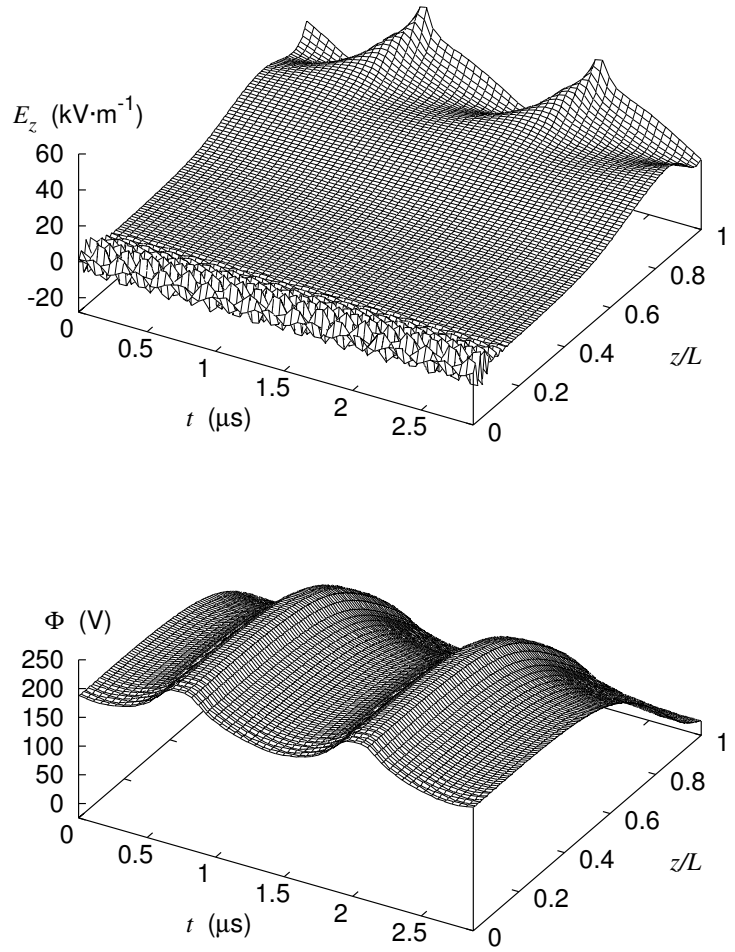

FIGURE 4: Simulated transit-time oscillations of electric field and plasma potential from simulations for a prescribed discharge current ($I_d = 3\,\mathrm{A}$) in the same conditions as in figure 1. The reference potential is taken in the exit plane.

There exists an apparent inconsistency between the proposed dispersion relation and the statement made in references [1, 2] that the transit-time instability is associated with a standing wave. Contrasting the evolution of the simulated electric field and electric potential (figure 4), however, it seems very possible that the experimental data, which consisted uniquely in plasma potential measurements, were misinterpreted. Although it is clear from the electric field profile that the wave is a traveling one, the plasma potential fluctuations can be easily mistaken for standing waves due to the fact that the potential does not characterize only the local state but the whole plasma column between the measurement point and the reference point.

5.2 Comparison with the numerical model

The low ionization criterion (36) synthesized by figure 3 predicts two unstable regions: a low-Mach/low ionization degree region where the ion velocity can be negative, and a high-Mach region where the ionization degree can be large.

These results are consistent with the observations made with the numerical model, where both the reverse ion flow region close to anode ($I_i < 0$, $|I_i| \ll I_d$) and the acceleration region close to the exhaust plane ($\mathcal{M}_i > 1$) are potentially unstable (figure 1). The prediction that almost the whole supersonic region is subjected to

transit-time oscillations when the ionization degree is high is also consistent with the behavior of the fluid model. Finally, the fact that the reverse ion flow region is seldom affected by the instability might be explained by the stabilizing effect of ionization, highlighted by the low-Mach stability criterion (37).

As mentioned in section 4.3, transit-time oscillations are expected to present a broad frequency spectrum. By contrast, numerical models show very coherent oscillations with a very narrow frequency spectrum. It must be remembered, however, that numerical models present a non-negligible level of artificial diffusion, which acts essentially as ξ in the equation system (29, 30). Therefore, high frequencies are strongly damped and the frequency associated with the smallest wavenumber dominates.

5.3 Feedback mechanisms

The fact that a region is unstable does not necessarily means that it will be spontaneously subjected to oscillations. Since the unstable waves are convected away, a feedback mechanism must also be present for the mode to be self-excited.

Some of the possible mechanisms potentially able to retro-propagate information are:

1. ion acoustic waves, which propagate with velocities $V_{iz} \pm C_s$,
2. the discharge current, which propagates almost instantaneously across the discharge interval,
3. electron energy, which is transported at the velocity V_{ez}.

The first mechanism is clearly a good candidate to explain the self-excited oscillations observed in the subsonic region. In the supersonic region, however, the acoustic waves are both convected towards exit and cannot carry information back into the channel. Simulations confirm that either the discharge current or the electron energy can provide feedback in the supersonic region: if both of these mechanisms are disabled (*e.g.* by taking a constant discharge current and a local electron energy equation), the transit-time oscillations die out.

5.4 Suppression of transit-time instabilities in numerical models

Modern Hall thrusters do not seem to be subjected to transit-time oscillations, even though these are often predicted by numerical models. A possible explanation for this discrepancy is that the physical diffusion/dissipation processes neglected in numerical models could provide a strong damping, as suggested by equation (31). Actually, even in numerical models the level of transit-time oscillations is very dependent upon the amount of numerical diffusion, and for this reason these oscillations are not weak [11] or totally absent [12] in models using first-order accurate schemes. The (incorrect) prediction of transit-time oscillations is thus paradoxically the consequence of a high numerical accuracy.

The damping of transit-time oscillations can be achieved by introducing a slight amount of artificial diffusion in the numerical scheme, for instance by solving an equation system similar to (29, 30). In order to add as little artificial diffusion as possible, it is preferable to adapt ξ to the potential magnitude of the growth rate. Since the growth rate is a function of the Mach number, the empirical expression

$$\xi = L_d C_s \left(1 + \mathcal{M}_i^2\right) \tag{38}$$

was used in the fluid model, and seems to constitute a sensible and reasonably universal weight for most cases. A diffusion length $L_d = 0.1 - 0.2\,\text{mm}$ was found to be in general sufficient to fully suppress transit-time oscillations. For such low values of L_d, no sensible impact was observed on either the stationary profiles or on the low-frequency oscillations (this was verified by comparing the solution obtained with $L_d = L_d^*$ and $L_d = 2L_d^*$, where L_d^* is the critical value for which transit-time oscillations are fully damped).

In future developments, we shall hopefully propose a more optimal expression of the artificial viscosity where the ionization degree is taken into account.

6 Conclusion

A new theory of transit-time oscillations has been proposed which seems to properly explain the location of the unstable regions observed in a fluid model of Hall thrusters. Two potentially unstable regions were identified, close to the anode and in the acceleration zone.

Several of the predicted characteristics seem to confirm the presumed relationship between the numerical transit-time instability and the transit-time instability found in experiments, namely:

- the instability is more probable at high ionization degrees,
- the frequency roughly scales with the acoustic propagation velocity ($V_i \pm C_s$),
- the behavior of the growth at high frequencies predicts a wide frequency spectrum.

Besides, the high likelihood for unstable modes in numerical models was attributed to the probable neglect of physical small-scale diffusion processes. Acknowledging that transit-time oscillations are not observed in modern Hall thrusters, the introduction of artificial diffusion was proposed as an efficient way to damp unstable modes.

Acknowledgements

This work was done within the frame of the French Research Group "Plasma Propulsion for Space Systems" (GDR No 2232 CNRS/CNES/SNECMA/ONERA). S. Barral and K. Makowski also wish to acknowledge the support given by the Polish Committee for Scientific Research (KBN) in the frame of the project 8-T12D-015-21. The authors thank J.-P. Boeuf and L. Garrigues for fruitful discussions that inspired several aspects of this work.

[1] A. I. Morozov, Yu. Esipchuck, A. M. Kapulkin, V. A. Nevrovskii, and V. A. Smirnov. Azimuthally asymmetric modes and anomalous conductivity in closed electron drift accelerators. *Sov. Phys. Tech. Phys.*, 18:615, 1973.

[2] Yu. B. Esipchuk, A. I. Morozov, G. N. Tilinin, and A. V. Trofimov. Plasma oscillations in closed-drift accelerators with an extended acceleration zone. *Sov. Phys. Tech. Phys.*, 18:928, 1974.

[3] J. M. Fife. Two-dimensional hybrid particle-in-cell modeling of Hall thrusters. Master's thesis, Massachusetts Institute of Technology, 1995.

[4] L. Garrigues, A. Héron, J.-C. Adam, and J.-P. Boeuf. Hybrid and particle-in-cell models of a stationary plasma thruster. *Plasma Sources Sci. Technol.*, 9:219, 2000.

[5] G. J. M. Hagelaar, J. Bareilles, L. Garrigues, and J.-P. Boeuf. Role of anomalous electron transport in a stationary plasma thruster simulation. *J. Appl. Phys.*, 93:67, 2003.

[6] S. Barral. *Numerical Studies of Hall Thrusters Based on Fluid Equations for Plasma*. PhD thesis, Institute of Fundamental Technological Research of Warsaw, 2003.

[7] Yu. B. Esipchuk and G. N. Tilinin. Drift instability in a Hall-current plasma accelerator. *Sov. Phys. Tech. Phys.*, 21:417, 1976.

[8] V. I. Baranov, Yu. S. Nazarenko, V. A. Petrosov, A. I. Vasin, and Yu. M. Yashnov. New conception of oscillation mechanisms in the accelerators with closed drift of electrons. In *Proc. 24th International Electric Propulsion Conference*, number 95-044, Moscow, 1995.

[9] S. Barral, K. Makowski, Z. Peradzyński, and M. Dudeck. Model of stationary plasma thruster with conducting walls. In *Proc. 38th AIAA Joint Propulsion Conference*, number 2002-4245, Indianapolis, 2002.

[10] S. Barral, K. Makowski, Z. Peradzyński, N. Gascon, and M. Dudeck. Wall material effects in stationary plasma thrusters; part II: Wall conductivity theory. Submitted to Phys. Plasmas.

[11] J.-P. Boeuf and L. Garrigues. Low frequency oscillations in a stationary plasma thruster. *J. Appl. Phys.*, 84:3541, 1998.

[12] K. Makowski, S. Barral, Z. Peradzyński, and M. Dudeck. Influence of the plasma-wall interactions on the operation of Hall thrusters. In *Proc. 3rd International Conference on Spacecraft Propulsion*, page 377, Cannes (France), 2000.